The Tensor Formulation of Ferromagnetic Resonance

J. A. YOUNG, JR.,* AND EDWIN A. UEHLING
University of Washington, Seattle, Washington
(Received December 7, 1953)

The tensor formulation of electromagnetic wave propagation in a conducting ferromagnetic medium is used to describe resonance phenomena in a test cavity under two different conditions of magnetization. The new formulation alters the prediction with respect to the shape of the resonance curve in the case of perpendicular magnetization and it predicts a different ratio of energy absorptions in the cases of parallel and perpendicular magnetization than is given by a formulation based on the concept of a permeability coefficient. When interpreted according to the new formulation the results of simultaneous measurements of frequency shift and energy absorption under different conditions of magnetization are found to be consistent with each other. Such consistency is not achieved on the basis of earlier formulations.

I. INTRODUCTION

IT has been reported previously[1] that the theory of ferromagnetic resonance based on the concept of a complex permeability coefficient is unable to explain the experimental data under all conditions of magnetization. Using a reflection type cavity with a ferromagnetic metal as one wall of that cavity we obtained results for the absorption, frequency shift, and the shape of resonance curves under two conditions of magnetization; namely, (a) the applied constant magnetic field is parallel to the surface of the ferromagnetic sample; and, (b) it is perpendicular to that surface. These conditions are frequently called the conditions of parallel and perpendicular magnetization, respectively, and we will use this terminology here. The important discrepancies observed were in the shape of the resonance curves for the case of perpendicular magnetization and in the ratio of absorptions in the two cases of parallel and perpendicular magnetization.

These discrepancies were to a large extent resolved by employing the concept of a permeability tensor first introduced by Polder.[2] A consistent application of this concept shows that only in the case of parallel magnetization is the concept of a permeability coefficient equivalent to that of a tensor. In all other cases the usual theory employing the permeability coefficient gives incorrect results.

At first sight these conclusions may appear somewhat surprising in view of the fact that Polder demonstrated the equivalence of the two formulations for the nonmetals insofar as the relation between fields and magnetization is concerned. The conditions for equivalence are that the sample dimensions be small compared with the wavelength and that the displacement currents be negligible, both of which are fulfilled in our experiments. We will again demonstrate this equivalence, but we will also show that in the parallel resonance case it is a consequence of a definite relation between the longitudinal and transverse components of the magnetic field in that part of the wave which is polarized perpendicular to the constant field, whereas, in the case of perpendicular magnetization, there is in general no such relation between magnetic field components because the two waves of opposite directions of circular polarization are essentially independent.

The theoretical problem will be formulated in Sec. II. The description of magnetic resonance phenomena will be based as usual on the phenomenological equations, and the usual restrictions to the case of saturation magnetization in ferromagnetic samples and vanishingly small alternating fields will be made. The final equations which express the quality factor Q and the frequency shift $\Delta\omega$ of the cavity in terms of the properties of the ferromagnetic medium, the frequency of the oscillating fields and the value of the applied constant magnetic field will be given at the end of this section for both the case of parallel and perpendicular magnetization and for the two commonly considered types of damping. In writing these equations we specialize to the case of metals. It is a simple matter to rewrite them for the case of semiconducting ferromagnetic media.

The remainder of the paper is devoted to a discussion of the experimental conditions under which our data on a few carefully chosen samples of nickel and supermalloy were obtained, and to a comparison of the results obtained with the theoretical predictions. The experimental conditions and the methods which we used to relate theory and experiment are described in Sec. III. Finally, in Sec. IV we discuss the experimental results. Using the theoretical formulation given in Sec. II we find that the case of perpendicular resonance is as adequately described by the theory as is the case of parallel resonance. Consequently, we have some confidence in the validity of comparisons of the results obtained under these two different experimental conditions. The principal conclusion which we are able to draw from this comparison is that the Landau-Lifshitz type of damping is not nearly as satisfactory as the Bloch type. Both of course lead to an essentially Lorentz type of resonance curve, but the Landau-Lifshitz damping introduces terms into the permeability tensor compo-

* Now at the Bell Telephone Laboratories, Holmdel, New Jersey.

[1] J. A. Young, Jr., and Edwin A. Uehling, Phys. Rev. **90**, 990 (1953).

[2] D. Polder, Phil. Mag. **40**, 99 (1949).

nents which have no Bloch counterpart and which on *a priori* grounds appear to be physically meaningless. Consequently, it is satisfying to find the data leading to the conclusion which we obtain. The conclusion appears to be unambiguous, but one would like to have an additional test at another frequency than the one of 9000 Mc/sec which we used.

Small discrepancies between theory and experiment still remain. We believe that these discrepancies lie outside of our experimental errors. These discrepancies are discussed briefly.

II. THE RESONANCE EQUATIONS

We will analyze the problem of absorption in a rectangular cavity in which one wall of the cavity consists of the ferromagnetic material under test. According to the methods first introduced by Polder[2] and subsequently applied to particular cases by Hogan[3] and Weiss and Fox[4] we begin the analysis by consideration of the propagation properties in a ferromagnetic medium of infinite extent. Magnetic phenomena in such a medium may be described by the well-known phenomenological equations[5]:

$$\dot{M}_{x,y}=\gamma[\mathbf{M}\times\mathbf{H}]_{x,y}-M_{x,y}/T_2, \tag{1}$$

for Bloch (B-type) damping, and

$$\begin{aligned}\dot{M}_{x,y}&=\gamma[\mathbf{M}\times\mathbf{H}]_{x,y}-\frac{\alpha\gamma}{|M|}[\mathbf{M}\times[\mathbf{M}\times\mathbf{H}]]_{x,y}\\&\cong\gamma[\mathbf{M}\times\mathbf{H}]_{x,y}-\alpha\gamma(H_zM_{x,y}-M_0H_{x,y}),\end{aligned} \tag{2}$$

for Landau-Lifshitz (LL-type) damping, where we have already used the fact that the applied constant magnetic field is to be taken in the z direction and that this field is sufficiently strong to produce a saturation magnetization M_0. Also, $\gamma=ge/2mc$ is the gyromagnetic ratio of the electrons which provide the magnetization, T_2 is the transverse relaxation time of Bloch, α is the damping parameter of Landau-Lifshitz, $\mathbf{M}$ is the magnetization vector, and $\mathbf{H}$ is the applied field. We now denote the constant magnetic field in the z direction by H_0. In addition we apply an oscillating magnetic field in the xy plane of components h_x and h_y of frequency ω. Then we solve (1) and (2) after introducing:

$$\begin{aligned}&H_x=h_xe^{j\omega t}, &&M_x=m_xe^{j\omega t},\\&H_y=h_ye^{j\omega t}, &&M_y=m_ye^{j\omega t},\\&H_z=H_0-N_zM_0,\end{aligned}$$

where N_z is a demagnetization factor which we must use in connection with the applied constant field. No other demagnetizing factors are used. We then obtain:

$$m_x=\frac{\gamma^2M_0(H_0-N_zM_0)h_x-\gamma M_0(j\omega+1/T_2)h_y}{\gamma^2(H_0-N_zM_0)^2+(j\omega+1/T_2)^2}, \tag{3a}$$

$$m_y=\frac{\gamma M_0(j\omega+1/T_2)h_x+\gamma^2M_0(H_0-N_zM_0)h_y}{\gamma^2(H_0-N_zM_0)^2+(j\omega+1/T_2)^2}, \tag{3b}$$

for the case of B-type damping, and

$$m_x=\frac{\gamma M_0\{\gamma(H_0-N_zM_0)+\alpha[j\omega+\alpha\gamma(H_0-N_zM_0)]\}h_x-j\omega\gamma M_0h_y}{\gamma^2(H_0-N_zM_0)^2+[j\omega+\alpha\gamma(H_0-N_zM_0)]^2}, \tag{4a}$$

$$m_y=\frac{\gamma M_0\{\gamma(H_0-N_zM_0)+\alpha[j\omega+\alpha\gamma(H_0-N_zM_0)]\}h_y+j\omega\gamma M_0h_x}{\gamma^2(H_0-N_zM_0)^2+[j\omega+\alpha\gamma(H_0-N_zM_0)]^2}, \tag{4b}$$

for the case of LL-type damping.

The magnetic induction is

$$\mathbf{B}=\mathbf{b}e^{j\omega t},$$

where

$$\mathbf{b}=\mathbf{h}+4\pi\mathbf{m}.$$

Thus, we find Eqs. (3) and (4) are consistent with the relations:

$$b_x=\mu h_x-jKh_y, \quad b_y=jKh_x+\mu h_y, \quad b_z=h_z, \tag{5}$$

in which

$$\mu=1+\frac{4\pi\gamma^2M_0(H_0-N_zM_0)}{\gamma^2(H_0-N_zM_0)^2+[j\omega+(1/T_2)]^2}, \tag{6a}$$

$$K=-j\frac{4\pi\gamma M_0[j\omega+(1/T_2)]}{\gamma^2(H_0-N_zM_0)^2+[j\omega+(1/T_2)]^2}, \tag{6b}$$

for B-type damping, and

$$\mu=1+\frac{4\pi\gamma M_0\{\gamma(H_0-N_zM_0)+\alpha[j\omega+\alpha\gamma(H_0-N_zM_0)]\}}{\gamma^2(H_0-N_zM_0)^2+[j\omega+\alpha\gamma(H_0-N_zM_0)]^2}, \tag{7a}$$

$$K=\frac{4\pi\gamma\omega M_0}{\gamma^2(H_0-N_zM_0)^2+[j\omega+\alpha\gamma(H_0-N_zM_0)]^2}, \tag{7b}$$

for LL-type damping.

Our next step is to obtain plane wave solutions of the Maxwell equations:

$$\nabla\times\mathbf{e}=-(1/c)\dot{\mathbf{b}}, \quad \nabla\times\mathbf{h}=(4\pi\sigma/c)\mathbf{e}+(1/c)\dot{\mathbf{d}}, \tag{8}$$

which are of the form:

$$\begin{aligned}&\mathbf{b}=\mathbf{b}_0\exp[j\omega t-P(\mathbf{n}\cdot\mathbf{r})],\\&\mathbf{h}=\mathbf{h}_0\exp[j\omega t-P(\mathbf{n}\cdot\mathbf{r})],\\&\mathbf{e}=\mathbf{e}_0\exp[j\omega t-P(\mathbf{n}\cdot\mathbf{r})],\\&\mathbf{d}=\epsilon\mathbf{e}.\end{aligned} \tag{9}$$

[3] C. L. Hogan, Bell System Tech. J. **31**, 1 (1952).
[4] M. T. Weiss and A. G. Fox, Phys. Rev. **88**, 146 (1952).
[5] C. Kittel, Phys. Rev. **73**, 155 (1948); N. Bloembergen, Phys. Rev. **78**, 572 (1950) for applications using Bloch type damping; Yager, Galt, Merritt, and Wood, Phys. Rev. **80**, 744 (1950) for applications using Landau-Lifshitz type damping.

The substitution of Eqs. (9) into (8) leads to:

$$P[\mathbf{e}_0\times\mathbf{n}]=-j\omega\mathbf{b}_0/c,\quad P[\mathbf{h}_0\times\mathbf{n}]=(4\pi\sigma+j\omega\epsilon)\mathbf{e}_0/c.$$

We obtain a relation between $\mathbf{b}_0$ and $\mathbf{h}_0$ by eliminating $\mathbf{e}_0$ from these equations. Thus, we write the following equations connecting both $\mathbf{b}_0$ and $\mathbf{e}_0$ with $\mathbf{h}_0$

$$\lambda\mathbf{b}_0=P^2[\mathbf{n}(\mathbf{n}\cdot\mathbf{h}_0)-\mathbf{h}_0], \tag{10a}$$

$$\lambda c\mathbf{e}_0=-j\omega P[\mathbf{h}_0\times\mathbf{n}], \tag{10b}$$

where

$$\lambda=-j\omega(4\pi\sigma+j\omega\epsilon)/c^2. \tag{10c}$$

We now consider separately the two cases of propagation perpendicular to and parallel to the constant applied field H_0. From now on we drop the subscripts on **b**, **h**, and **e** since we will be working only with amplitudes.

(a) Propagation Perpendicular to H_0

We will take the direction of propagation as the y direction. Then,

$$n_x=n_z=0;\quad n_y=1.$$

We also use Eqs. (5). Thus, we find that Eqs. (10) have two independent solutions; namely,

$$\begin{aligned}&P^2=-\lambda,\\&e_y=e_z=h_x=h_y=0,\\&h_z\neq0\quad,\qquad e_x/h_z=j\omega P/\lambda c;\end{aligned} \tag{11}$$

and

$$\begin{aligned}&P^2=-\lambda(\mu^2-K^2)/\mu,\\&e_x=e_y=h_z=0,\\&h_y/h_x=-jK/\mu\quad,\qquad e_z/h_x=-j\omega P/\lambda c.\end{aligned} \tag{12}$$

The first case corresponds to propagation in a nonmagnetic medium. In the second case, the magnetic properties of the medium are contained in μ and K which are given by either Eqs. (6) or Eqs. (7).

(b) Propagation Parallel to H_0

Then $n_x=n_y=0$, $n_z=1$. Again using Eqs. (5) we find that Eqs. (10) have the two independent solutions:

$$\begin{aligned}&P^2=-\lambda(\mu\pm K),\\&h_z=e_z=0,\\&h_x/h_y=-e_y/e_x=\mp j,\\&e_y/h_x=-e_x/h_y=j\omega P/\lambda c,\end{aligned} \tag{13}$$

where the upper and lower signs correspond to the two directions of circular polarization, each with its own propagation constant, and where the magnetic properties of the medium are again contained in μ and K given by Eqs. (6) or (7).

We will now calculate the absorption and frequency shift in a cavity in which one wall consists of a ferromagnetic metal. Thus, we specialize the equations given above to the case of $\omega\epsilon/4\pi\sigma\ll1$ and consequently $\lambda=-4\pi j\omega\sigma/c^2$. The expressions for the quality factor Q and the frequency shift $\Delta\omega$ are conveniently determined from the equation[6]:

$$\frac{1}{Q}-2j\frac{\Delta\omega}{\omega}=\frac{c}{\omega}\frac{\int(\mathbf{n}\times\mathbf{e})\cdot\mathbf{h}_k dS}{\int\mathbf{h}\cdot\mathbf{h}_k dV}, \tag{14}$$

where $\mathbf{e}_k$ and $\mathbf{h}_k$ are the normalized unperturbed electric and magnetic fields within the cavity for the mode k in which the cavity is considered to be oscillating, $\int dS$ is the integral over the bounding surfaces of the cavity, and $\int dV$ is the integral over the cavity volume. The equation of reference 6 from which (14) is taken has been specialized here to the case of a cavity all of whose walls are conducting, and we have used in addition the relation:

$$\int\mathbf{e}\cdot\mathbf{e}_k dV=-j\int\mathbf{h}\cdot\mathbf{h}_k dV.$$

The equation is expressed in Gaussian units to agree with our other equations.

We will evaluate the integrals in Eq. (14) for each of the two cases of parallel and perpendicular magnetization.

(1) *Parallel Magnetization*

The xz plane lies in the surface of the ferromagnetic specimen with the constant magnetic field H_0 directed along the z axis. The direction of propagation is along the y axis which is normal to the surface and directed outward from the cavity. The magnetic vector **h** is linearly polarized and the direction of polarization makes an angle θ with H_0. Then from Eqs. (11) and (12) we have:

$$\begin{aligned}&P=P_0=(-\lambda)^{\frac{1}{2}}=(1+j)(2\pi\omega\sigma)^{\frac{1}{2}}/c,\\&e_x=j\omega P_0 h_z/\lambda c=-cP_0 h\cos\theta/4\pi\sigma,\end{aligned} \tag{15}$$

for the component of **h** along the z axis, and

$$\begin{aligned}&P=(-\lambda(\mu^2-K^2)/\mu)^{\frac{1}{2}}=(1+j)(2\pi\omega\sigma)^{\frac{1}{2}}((\mu^2-K^2)/\mu)^{\frac{1}{2}}/c,\\&e_z=-j\omega Ph_x/\lambda c=cPh\sin\theta/4\pi\sigma,\end{aligned} \tag{16}$$

for the component of **h** along the x axis. Since $\mathbf{n}=\mathbf{j}$,

$$[\mathbf{n}\times\mathbf{e}]=ch(\mathbf{i}P\sin\theta+\mathbf{k}P_0\cos\theta)/4\pi\sigma.$$

We regard the unperturbed cavity oscillation as taking

[6] J. C. Slater, Revs. Modern Phys. 18, 441 (1946), especially Eq. III.53, p. 475.

place in a single mode k. Then

$$\mathbf{h}=\mathbf{h}_k\int\mathbf{h}\cdot\mathbf{h}_k dV,$$

$$[\mathbf{n}\times\mathbf{e}]\cdot\mathbf{h}_k=\frac{c}{4\pi\sigma}hh_k(P\sin^2\theta+P_0\cos^2\theta)$$

$$=\frac{c}{4\pi\sigma}h_k^2(P\sin^2\theta+P_0\cos^2\theta)\int\mathbf{h}\cdot\mathbf{h}_k dV,$$

$$\int[\mathbf{n}\times\mathbf{e}]\cdot\mathbf{h}_k dS\Big/\int\mathbf{h}\cdot\mathbf{h}_k dV$$

$$=\frac{c}{4\pi\sigma}(P\sin^2\theta+P_0\cos^2\theta)\int h_k^2 dS.$$

Then for parallel magnetization:

$$\frac{1}{Q}-2j\frac{\Delta\omega}{\omega}=\frac{c^2}{4\pi\omega\sigma}(P\sin^2\theta+P_0\cos^2\theta)\int h_k^2 dS.$$

We define $1/Q_0$ as the real part of the right member of this equation when $\mu=1$ and $K=0$. Then,

$$\frac{1}{Q}-2j\frac{\Delta\omega}{\omega}=\frac{1}{Q_0}\frac{c}{(2\pi\omega\sigma)^{\frac{1}{2}}}(P\sin^2\theta+P_0\cos^2\theta). \quad (17)$$

(2) *Perpendicular Magnetization*

The z axis is now normal to the surface of the ferromagnetic specimen and is directed outward from the cavity. It is both the direction of H_0 and the direction of wave propagation. Take the x axis as the axis of the linearly polarized unperturbed magnetic vector $\mathbf{h}$ at the surface of the cavity. The wave propagates into the medium as two independent waves of + and − directions of circular polarizations. From Eqs. (13) and the condition of linear polarization at the surface,

$$\begin{aligned}
&h_x=h_x^+ + h_x^-, \quad \text{where} \quad h_x^+=h_x^-;\\
&h_y=h_y^+ + h_y^-=jh_x^+ - jh_x^-=0,\\
&e_x=e_x^+ + e_x^-=\omega(P^+-P^-)h_x/2\lambda c,\\
&e_y=e_y^+ + e_y^-=j\omega(P^++P^-)h_x/2\lambda c,\\
&P^+=(-\lambda(\mu+K))^{\frac{1}{2}},\\
&P^-=(-\lambda(\mu-K))^{\frac{1}{2}}, \quad \text{where} \quad \lambda=-4\pi j\omega\sigma/c^2.
\end{aligned} \quad (18)$$

Since $\mathbf{n}=\mathbf{k}$ and $\mathbf{h}=\mathbf{h}_k\int\mathbf{h}\cdot\mathbf{h}_k dV$, where $\mathbf{h}=\mathbf{i}h_x=\mathbf{i}h$, we have:

$$[\mathbf{n}\times\mathbf{e}]\cdot\mathbf{h}_k=-\frac{j\omega h_k^2}{2\lambda c}(P^++P^-)\int\mathbf{h}\cdot\mathbf{h}_k dV,$$

$$\int[\mathbf{n}\times\mathbf{e}]\cdot\mathbf{h}_k dS\Big/\int\mathbf{h}\cdot\mathbf{h}_k dV=-\frac{j\omega}{2\lambda c}(P^++P^-)\int h_k^2 dS$$

$$=\frac{c}{8\pi\sigma}(P^++P^-)\int h_k^2 dS.$$

Thus for perpendicular magnetization:

$$\frac{1}{Q}-2j\frac{\Delta\omega}{\omega}=\frac{c^2}{8\pi\omega\sigma}(P^++P^-)\int h_k^2 dS.$$

Defining Q_0 as before, we obtain:

$$\frac{1}{Q}-2j\frac{\Delta\omega}{\omega}=\frac{1}{Q_0}\frac{c}{(8\pi\omega\sigma)^{\frac{1}{2}}}(P^++P^-). \quad (19)$$

We will now evaluate the propagation constants using the previously derived expressions for μ and K. Again we consider separately the two cases of parallel and perpendicular magnetization.

(3) *Parallel Magnetization*

Using Eqs. (6a), (6b), (7a), and (7b) with N_z set equal to zero we obtain:

$$\mu^2-K^2/\mu=\mu_1-j\mu_2, \quad (20)$$

where

$$\mu_1=1+\frac{4\pi\gamma^2M_0(H_0+4\pi M_0)(\omega_0^2-\omega^2)}{(\omega_0^2-\omega^2)^2+4\omega^2/T_2^2}, \quad (21a)$$

$$\mu_2=\frac{4\pi\gamma^2M_0(H_0+4\pi M_0)}{(\omega_0^2-\omega^2)^2+4\omega^2/T_2^2}\frac{2\omega}{T_2}, \quad (21b)$$

$$\omega_0^2=\gamma^2H_0(H_0+4\pi M_0)+1/T_2^2, \quad (21c)$$

for the case of B-type damping; and

$$\mu_1=1+4\pi\gamma^2M_0\frac{(H_0+4\pi M_0)(1+\alpha^2)(\omega_0^2-\omega^2)+\alpha^2\omega^2(2H_0+4\pi M_0)}{(\omega_0^2-\omega^2)^2+\omega^2\alpha^2\gamma^2(2H_0+4\pi M_0)^2}, \quad (22a)$$

$$\mu_2=4\pi\gamma M_0\alpha\omega\frac{\gamma^2(H_0+4\pi M_0)^2(1+\alpha^2)+\omega^2}{(\omega_0^2-\omega^2)^2+\omega^2\alpha^2\gamma^2(2H_0+4\pi M_0)^2}, \quad (22b)$$

$$\omega_0^2=\gamma^2H_0(H_0+4\pi M_0)(1+\alpha^2), \quad (22c)$$

for the case of LL-type damping. These results for μ_1 and μ_2 are identical with the expressions for the real and imaginary parts of the complex permeability coefficient which have been previously derived from the point of view of demagnetizing factors.[7]

Combining Eqs. (16) and (20), we have:

$$P^2=4\pi j\omega\sigma(\mu_1-j\mu_2)/c^2. \quad (23)$$

If we set $P=P_1+jP_2$, we obtain:

$$P_1=(2\pi\omega\sigma\mu_R)^{\frac{1}{2}}/c, \quad P_2(\pm)(2\pi\omega\sigma\mu_L)^{\frac{1}{2}}/c, \quad (24)$$

where

$$\mu_R=(\mu_1^2+\mu_2^2)^{\frac{1}{2}}+\mu_2, \quad \mu_L=(\mu_1^2+\mu_2^2)^{\frac{1}{2}}-\mu_2. \quad (25)$$

[7] See for example Eqs. (10) and (11) of reference 11 and Eqs. (A-2) and (A-3) in the paper of Yager *et al.* of reference 5, which are the same as our Eqs. (21a and b) and (22a and b) if in the former $N_x=N_z=0$ and $N_y=4\pi$ corresponding to the case of parallel magnetization.

We will use $(\pm)$ inclosed in parentheses to signify that the positive or negative value is to be taken according to whether the real quantity μ_1 is positive or negative. P_0 is obtained by setting $\mu_1=1$ and $\mu_2=0$. Substitution into Eq. (17) then gives us the final results for the parallel resonant case:

$$\frac{1}{Q}=\frac{1}{Q_0}[(\mu_R)^{\frac{1}{2}}\sin^2\theta+\cos^2\theta], \tag{26a}$$

$$-\frac{2\Delta\omega}{\omega}=\frac{1}{Q_0}[(\pm)(\mu_L)^{\frac{1}{2}}\sin^2\theta+\cos^2\theta]. \tag{26b}$$

(4) *Perpendicular Magnetization*

Using Eqs. (6a), (6b), (7a), and (7b) with N_z set equal to 4π, we obtain

$$\mu\pm K=\mu_1{}^{\pm}-j\mu_2{}^{\pm}, \tag{27}$$

where

$$\mu_1{}^{\pm}=1+\frac{4\pi\gamma M_0(\omega_0\mp\omega)}{(\omega_0\mp\omega)^2+1/T_2{}^2}, \tag{28a}$$

$$\mu_2{}^{\pm}=\pm\frac{4\pi\gamma M_0/T_2}{(\omega_0\mp\omega)^2+1/T_2{}^2}, \tag{28b}$$

$$\omega_0=\gamma(H_0-4\pi M_0), \tag{28c}$$

for the case of B-type damping; and

$$\mu_1{}^{\pm}=1+\frac{4\pi\gamma M_0(\omega_0\mp\omega+\alpha^2\omega_0)}{(\omega_0\mp\omega)^2+\alpha^2\omega_0{}^2}, \tag{29a}$$

$$\mu_2{}^{\pm}=\frac{4\pi\gamma M_0\alpha\omega}{(\omega_0\mp\omega)^2+\alpha^2\omega_0{}^2}, \tag{29b}$$

$$\omega_0=\gamma(H_0-4\pi M_0), \tag{29c}$$

for LL-type damping. In contrast with the case of parallel magnetization these expressions for $\mu_1{}^{\pm}$ and $\mu_2{}^{\pm}$ bear little resemblance to the real and imaginary parts of the permeability coefficient as previously derived on the basis of demagnetization factors.

Combining Eqs. (18) and (27), we have:

$$(P^{\pm})^2=4\pi j\omega\sigma(\mu_1{}^{\pm}-j\mu_2{}^{\pm})/c^2. \tag{30}$$

If we set $P^{\pm}=P_1{}^{\pm}+jP_2{}^{\pm}$, we obtain:

$$P_1{}^{\pm}=(2\pi\omega\sigma\mu_R{}^{\pm})^{\frac{1}{2}}/c, \quad P_2{}^{\pm}=(\pm)(2\pi\omega\sigma\mu_L{}^{\pm})^{\frac{1}{2}}/c, \tag{31}$$

where

$$\begin{aligned}\mu_R{}^{\pm}&=(\mu_1{}^{\pm 2}+\mu_2{}^{\pm 2})^{\frac{1}{2}}+\mu_2{}^{\pm},\\ \mu_L{}^{\pm}&=(\mu_1{}^{\pm 2}+\mu_2{}^{\pm 2})^{\frac{1}{2}}-\mu_2{}^{\pm},\end{aligned} \tag{32}$$

and the factor $(\pm)$ denotes that $P_2{}^{+}$ has the same sign as $\mu_1{}^{+}$. Since $\mu_1{}^{-}$ is always positive, $P_2{}^{-}$ is always positive.

Substitution into Eq. (19) gives the final results for the case of perpendicular magnetization:

$$\frac{1}{Q}=\frac{1}{2Q_0}[(\mu_R{}^{+})^{\frac{1}{2}}+(\mu_R{}^{-})^{\frac{1}{2}}], \tag{33a}$$

$$-\frac{2\Delta\omega}{\omega}=\frac{1}{2Q_0}[(\pm)(\mu_L{}^{+})^{\frac{1}{2}}+(\mu_L{}^{-})^{\frac{1}{2}}]. \tag{33b}$$

Equations (26a and b) and (33a and b), together with the immediately preceding defining equations, represent the final results of the analysis to which the experimental results presented in the next two sections will be referred.

We will conclude this section with some remarks concerning the equivalence and lack of equivalence of results based on the concept of the permeability tensor as compared with results based on the concept of a permeability coefficient.

In the parallel field case we may have, according to Eq. (12), two independent waves in which the magnetic vectors are h_z and $h_y/h_x=-jK/\mu$, respectively. Thus according to Eq. (5) the magnetic induction is:

$$\begin{aligned}b_x&=\mu h_x-jKh_y=(\mu^2-K^2)h_x/\mu,\\ b_y&=jKh_x+\mu h_y=0,\\ b_z&=h_z.\end{aligned}$$

Thus the tensor relation is reduced to diagonal form, and, in particular, the coefficient relating b_x and h_x is, as we have stated immediately after Eqs. (20) to (22), just the permeability coefficient previously derived for the case of parallel magnetization using demagnetizing factors.

The situation is different in the case of perpendicular magnetization. According to Eq. (13) the components h_x and h_y within each of the two waves of $+$ and $-$ circular polarization are related by

$$h_x/h_y=\mp i,$$

but the two waves are independent of each other. If the amplitudes of the two waves are equal at the cavity surface they will not be equal within the ferromagnetic medium since the waves are attenuated differently. But we now see why Polder obtained the same results for magnetization as are given by a theory based on a permeability coefficient. If we set the amplitudes of the two waves equal, i.e., $h_x{}^{+}=h_x{}^{-}$, it follows that $h_y=0$. Then, according to Eq. (5),

$$b_x=\mu h_x,$$

where μ is given by Eq. (6a) or (7a). These expressions for μ are precisely the permeability coefficients previously derived if in the latter we set all demagnetizing factors except N_z equal to zero and take $N_z=4\pi$ to correspond to this case of perpendicular magnetization.[8]

[8] The previously derived results are given by the equations quoted in reference 7. In order to make the comparison, the definition of ω_0 given in Eqs. (28c) or (29c) must be used.

We observe that $\mu_R^{\pm}$ and $\mu_L^{\pm}$ in Eqs. (33a and b) are different functions of the frequencies and material properties than μ_R and μ_L in Eqs. (26a and b). Consequently, the correct expressions for the perpendicular case differ from those previously used not merely in the appearance of the factor $\frac{1}{2}$, corresponding to the fact that most of the loss is in only one of the two circularly polarized waves, but also in the actual forms of the loss factors.

III. EXPERIMENTAL METHODS

The experimental techniques and the methods of reducing data are similar to those used by others and described previously. Thin metallic foils of the ferromagnetic specimen form one end or side wall of a reflection-type cavity excited in the TE_{102} mode which terminates a wave-guide system and is coupled to it by an iris of suitable dimensions. The cavity is excited at its resonant frequency of approximately 9200 Mc/sec and the wave reflected from the cavity is led through a directional coupler to a detecting system. Detection is obtained by mixing the reflected signal with the modulated signal of a local oscillator in a manner similar to that described by Yager *et al.*[5] The magnetic field is current stabilized and variable over the range of 800 to 13 000 gauss. Its intensity is measured by determining the frequency of magnetic resonance of protons and lithium nuclei. The homogeneity of the field is such that the variation of field over the volume of the cavity is never more than $\frac{1}{2}$ gauss. Frequency stabilization of the source klystron is used. This is by means of a Pound-type cavity controlled circuit[9] with some improvements in the discrimination.[10] The resulting stability was within 1000 cps at 9200 Mc/sec. With the use of this equipment frequency changes of the order 0.02 Mc/sec could be measured with accuracy.

The experimental quantities which are measured are the resonance frequency and the reflection coefficient of the cavity under prescribed conditions of cavity coupling and magnetic state of the wall material. Actually we are interested in the change of frequency and the change of Q as a function of the magnetizing field at the ferromagnetic sample in the cavity. These quantities are given by Eqs. (26a and b) and (33a and b) in Sec. II and they have the form:

$$1/Q_{\text{fer}}=A/Q_0,$$
$$-2\Delta\omega_{\text{fer}}/\omega=B/Q_0,$$

where A and B are the theoretical quantities which are to be related to the experimental measurements. The methods for doing this have been discussed previously[11] and we will mention only certain modifications in the procedure.

The quantity $\Delta\omega_{\text{fer}}$ is measured directly and the only problem is the selection of a reference point. The quantity $1/Q_{\text{fer}}$ is obtained by a measurement of reflection coefficients at two points, one corresponding to the desired magnetic state of the ferromagnetic sample and the other a reference point. Denoting the reflection coefficient by Γ and using primes to indicate the reference point we can write:

$$A-A'=\frac{2Q_0}{Q_e}\frac{\Gamma'-\Gamma}{(1+\Gamma')(1+\Gamma)},$$

where Q_e is the contribution to the Q of the cavity which is due to the radiation of power from the cavity to the microwave system.

The two problems which must be solved in order to obtain useful experimental data are the determination of Q_e and Q_0 and the determination of suitable reference points.

Q_e is determined by a measurement of the frequency response curve of the cavity.[11] Q_0 is more difficult to determine. In accordance with the definition of Q_0 given in Sec. II immediately before Eq. (17), it may be calculated using the formula given there. This value is usually larger than the correct experimental value. However, Q_0 for our case is not easily measured since it is the nonmagnetic contribution of the portion of the cavity walls which are occupied by the ferromagnetic sample and the losses due to this wall are small compared with all other losses including the iris and clamping arrangements. However, we have shown that the clamping loss in our case is nearly constant since we were able to obtain a high degree of reproducibility of data obtained after assembly, dissassembly, and reassembly of the cavity. Also the effect of the iris on Q_0 is negligible as shown by experiments on the frequency shift using different irises. In our experiments Q_0 is finally determined as that quantity which provides consistency between theoretically and experimentally determined quantities under a large variety of conditions. In particular, one obtains a relation at resonance relating A, the reference value A', the measured Γ and Γ', the measured Q_e and a theoretical expression involving the parameter $\eta=2\pi\gamma M_0/\omega_0$ and the damping constant. ω_0 is measured and γ and M_0 are determined as the solutions of simultaneous equations for ω_0 corresponding to the two cases of parallel and perpendicular magnetization. The damping parameter is determined to provide the shape of curve which most nearly fits the experimental curve. Thus, in effect an actual value of Q_0 is not required, but results consistent with a single reasonable value of Q_0 are found.

The reference points are usually chosen to correspond to some value of the applied magnetic field which is sufficiently large so that A and B are effectively equal to unity independent of the nature or approximate

[9] R. V. Pound, Rev. Sci. Instr. **17**, 490 (1946) and Proc. Inst. Radio Engrs. **35**, 1405 (1947).

[10] Tuller, Galloway, and Zaffarno, Proc. Inst. Radio Engrs. **36**, 794 (1948).

[11] See, for example, N. Bloembergen, Phys. Rev. **78**, 572 (1950); a general discussion of these and other techniques is given in C. G. Montgomery, *Technique of Microwave Measurements*, MIT Radiation Laboratory Series (McGraw-Hill Book Company, Inc., New York, 1947), Vol. 11.

magnitude of the damping constant. We performed the the following experiments to determine whether or not this procedure is correct for our maximum field.

(a) With the sample on an end wall and the constant magnetic field parallel to the surface of the sample, revolution of the cavity through 90° about the axis of the wave guide can be made to bring the system from a position corresponding to that of parallel magnetization (constant magnetic field parallel to the surface of the specimen and perpendicular to the rf field) to a position of no magnetic effects (constant magnetic field parallel to the rf field). As shown by Eqs. (26a and b) with $\theta=0$ the last case corresponds strictly to $A=B=1$. Thus, the reference points are experimentally determined for the case of parallel magnetization at the same time that the data for this case is being obtained. It is true that one also observes certain small field effects in the so-called nonmagnetic orientation which are presumably due to the fact that θ is not exactly zero, as well as other effects of greater interest which are due presumably to the failure of the small field to saturate the sample. The latter requires special study but is not relevant to our discussions of reference points.

(b) With the sample on a side wall rotation about the wave-guide axis gives the difference between the cases of parallel and perpendicular magnetization. Having the reference points for the case of parallel magnetization one now obtains them for the case of perpendicular magnetization. Thus, the reference points for both cases are measured absolutely. The results for supermalloy using $H_0=13\,000$ gauss give the experimental values:

$$(\mu_R)^{\frac{1}{2}}=1.30 \quad \text{and} \quad (\mu_L)^{\frac{1}{2}}=1.22,$$

in the parallel field case, and

$$\tfrac{1}{2}[(\mu_R{}^+)^{\frac{1}{2}}+(\mu_R{}^-)^{\frac{1}{2}}]=1.78,$$
$$\tfrac{1}{2}[(\mu_L{}^+)^{\frac{1}{2}}+(\mu_L{}^-)^{\frac{1}{2}}]=1.42,$$

in the perpendicular field case. The calculated values from Eqs. (25) and (32) are 1.27 and 1.27 in the parallel field case and 1.74 and 1.71 in the perpendicular field case. Thus, we find that A and B are not equal to unity at the highest field available and we used, consequently, these procedures for the determination of the reference points.

TABLE I. Numerical values of g and $4\pi M_0$ for nickel, supermalloy, and 399 alloy.[a]

Material	g	$4\pi M_0$
Supermalloy	2.10	7770
Nickel	2.22	6170
399 alloy	2.28	5890

[a] The supermalloy samples were furnished by Dr. S. O. Morgan of the Bell Telephone Laboratories. The nickel samples were obtained from Baker and Company and are 99.5 percent pure. The 399 alloy is a Driver-Harris alloy of nickel and 0.2 percent silicon and with no contaminant greater than 0.05 percent.

One additional remark with regard to the experimental procedure should be made. Various sizes of iris were used. It may, for example, be chosen so that at the reference point the reflection coefficient is zero corresponding to critical coupling at this point. Under these conditions small effects are most accurately measured, and in particular, one obtains an accurate determination of the cavity frequency. If one now reduces the field and thus increases the loss in the cavity which is due to the approach to resonance of the ferromagnetic sample, the cavity becomes undercoupled (negative reflection coefficient Γ). But Γ may also approach unity in magnitude and since $A-A'$ is proportional to $(1+\Gamma)^{-1}$ the errors of measurement may become fairly large. In order to reduce these errors one then chooses an iris size so that the cavity is slightly overcoupled at the resonance point and the quantity $(1+\Gamma)$ is never permitted to be very much different from unity. We believe that the over-all error in our measurement of the reflection coefficient is not greater than 10 percent.

IV. RESULTS

In principle the complete determination of an absorption or a dispersion curve is sufficient to fix the numerical values of all relevant parameters. Since we are measuring both the absorption and dispersion, and since these measurements are being made for two different conditions of magnetization, all of our parameters are overstipulated. Thus, we obtain a rather stringent test of the adequacy of the theory to describe the phenomena in question.

Two of the parameters are rather easily determined independently of the nature of the theory used and independently of the nature and numerical value of the damping constant provided that it is small.[12] These are the saturation magnetization M_0 and the gyromagnetic ratio $\gamma=ge/2mc$. The resonance frequency for the case of parallel magnetization is given by Eqs. (21c) and (22c) in the cases of B- and LL-type damping, respectively, and by Eq. (28c) or (29c) in the case of perpendicular magnetization. Thus, e.g., in the case of B-type damping M_0 and γ are determined as the solutions of the two simultaneous equations:

$$\omega^2=\gamma^2H^{\parallel}(H^{\parallel}+4\pi M_0)+1/T_2{}^2, \quad \omega=\gamma(H^{\perp}-4\pi M_0),$$

where $H^{\parallel}$ and $H^{\perp}$ are the values of the constant magnetic field intensity at resonance in the cases of parallel and perpendicular magnetization, respectively. The principal source of error is in the determination of the resonant point. An error of ± 10 gauss in $H^{\parallel}$ and $H^{\perp}$ leads to an error of 35 gauss in $4\pi M_0$ and 0.03 in g. Our errors lie within these limits. The results which we have obtained as a consequence of a number of determinations on our samples are given in Table I.

One of the original objectives of these experiments

[12] Kittel, Yager, and Merritt, Physica 15, 256 (1949).

was to distinguish between the Bloch (B) and Landau-Lifshitz (LL) types of damping. Since both types lead to a Lorentz shape of curve it was expected that within the accuracy of the experiments it would be difficult to distinguish between the two damping mechanisms on the basis of line shape alone. Thus, Healy[13] has shown that he could fit his experimental curves equally well using either type of damping. But we expected that the ratio of absorptions in the two cases of parallel and perpendicular magnetizations would permit a distinction to be made. According to the usual theory of ferromagnetic resonance this ratio is independent of the numerical value of the damping constant but its dependence on the parameter $2\pi\gamma M_0/\omega_0$ is different in the two cases. Our experimental results differed from the predicted ratio in the most favorable case by a factor of about 1.5. In addition we observed that the shape of the resonance curve was correctly predicted only in the case of parallel magnetization,[14] but that in the case of perpendicular magnetization there were marked discrepancies.

These results may be interpreted to mean that neither type of damping mechanism is appropriate. However, the agreement between theory and experiment on line shape which is obtained in the case of parallel magnetization suggested the type of analysis which we have given in Sec. II, and it is now on the basis of this analysis that we will describe the experimental results obtained.

The experimental results will be presented under three headings:

(a) The ratio of absorption at resonance in the cases of parallel and perpendicular magnetizations.
(b) The over-all shape of resonance curves.
(c) Details in the shapes of resonance curves.

(a) Ratio of Absorptions at Resonance

In the case of parallel magnetization Eq. (26a) with $\theta=0$ gives

$$1/Q=(\mu_R)^{\frac{1}{2}}/Q_0.$$

At resonance we set $\mu_1\cong 0$ and we express H_0 in terms of ω_0 and other parameters. Making the substitution into $\mu_R\cong 2\mu_2$, we obtain:

$$\begin{aligned}(Q_0/Q)^2&=2\eta\omega_0T_2[\eta+(1+\eta^2)^{\frac{1}{2}}] \quad \text{B-type damping}\\ &=(2\eta/\alpha)[1+\eta(1+\eta^2)^{-\frac{1}{2}}] \quad \text{LL-type damping,} \quad (35)\end{aligned}$$

where

$$\eta=2\pi\gamma M_0/\omega_0.$$

[13] D. W. Healy, Phys. Rev. 86, 1009 (1952).
[14] As observed also by others; e.g., N. Bloembergen, reference 11; W. A. Yager, Phys. Rev. 75, 316 (1949); W. A. Yager and F. R. Merritt, Phys. Rev. 75, 318 (1949).

TABLE II. Experimental and theoretical values of $(Q_\perp/Q_\parallel)^2$ at resonance.

Specimen	Experimental	Eq. (39) (Usual theory based on a complex permeability coefficient) LL	B	Eq. (38) (Present theory based on a permeability tensor) LL	B
Nickel	4.1±0.4	1.7	2.5	2.6	3.8
Supermalloy	5.5±0.5	1.8	2.8	2.9	4.6

In the case of perpendicular magnetization we have, from Eq. (33a):

$$(1/Q)=(1/2Q_0)[(\mu_R^+)^{\frac{1}{2}}+(\mu_R^-)^{\frac{1}{2}}].$$

At resonance we set $\mu_1^+\cong 0$, $\mu_2^-\cong 0$ and substitute $H_0=\omega_0/\gamma+4\pi M_0$ into $\mu_R^+\cong 2\mu_2^+$ and $\mu_R^-\cong\mu_1^-$. We obtain:

$$\begin{aligned}\left(\frac{Q_0}{Q}\right)^2&=\eta\omega_0T_2\left[1+\frac{1}{2}\left(\frac{1+\eta}{\eta\omega_0T_2}\right)^{\frac{1}{2}}\right]^2 \quad \text{B-type damping}\\ &=\frac{\eta}{\alpha}\left[1+\frac{1}{2}\left(\alpha\frac{1+\eta}{\eta}\right)^{\frac{1}{2}}\right]^2 \quad \text{LL-type damping.} \quad (36)\end{aligned}$$

The usual theory in the case of parallel magnetization gives Eq. (35). In the case of perpendicular magnetization it gives:

$$\begin{aligned}(Q_0/Q)^2&=2\eta\omega_0T_2 \quad \text{B-type damping}\\ &=2\eta/\alpha \quad \text{LL-type damping,} \quad (37)\end{aligned}$$

where the values of μ_1 and μ_2 can be obtained from the equations quoted in reference 7 with N_z set equal to 4π to correspond to the case of perpendicular magnetization.

Taking the ratios of Q in the cases of parallel and perpendicular magnetization, we have:

$$\left(\frac{Q_\perp}{Q_\parallel}\right)^2=2[\eta+(1+\eta^2)^{\frac{1}{2}}]\left[1+\frac{1}{2}\left(\frac{1+\eta}{\eta\omega_0T_2}\right)^{\frac{1}{2}}\right]^{-2}$$

B-type damping

$$=2[1+\eta(1+\eta^2)^{-\frac{1}{2}}]\left[1+\frac{1}{2}\left(\alpha\frac{1+\eta}{\eta}\right)^{\frac{1}{2}}\right]^{-2}$$

LL-type damping, (38)

whereas the usual theory gives

$$\begin{aligned}\left(\frac{Q_\perp}{Q_\parallel}\right)^2&=\eta+(1+\eta^2)^{\frac{1}{2}} \quad \text{B-type damping}\\ &=1+\eta(1+\eta^2)^{-\frac{1}{2}} \quad \text{LL-type damping.} \quad (39)\end{aligned}$$

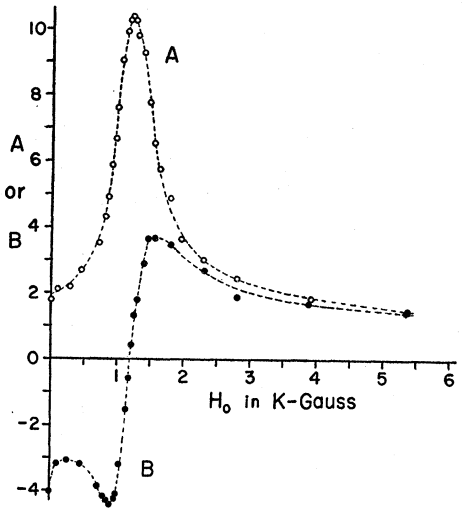

FIG. 1. Nickel parallel field case.

The parameter η is known from the experimental determinations leading to Table I. The parameters T_2 and α must be chosen to give the proper width of resonance curve. This cannot be done unambiguously to fit both the cases of parallel and perpendicular magnetization unless the type of damping used is actually the appropriate one. For our present purposes the quantities we are considering are relatively insensitive to the actual numerical value of the damping parameter. The comparisons which we now make are with $1/T_2=2.8\times10^9$ sec^{-1} and $\alpha=0.048$ for nickel and $1/T_2=1.7\times10^9$ sec^{-1} and $\alpha=0.029$ for supermalloy. Table II gives a tabulation of our experimental values of $(Q_\perp/Q_\parallel)^2$ together with the theoretical values calculated from Eqs. (38) and (39).

Thus, the theory of Sec. II gives results for the ratio of absorptions which is in fair agreement with the experimental values if Bloch damping is assumed. The remainder of the discussion will be based on only this type of damping.

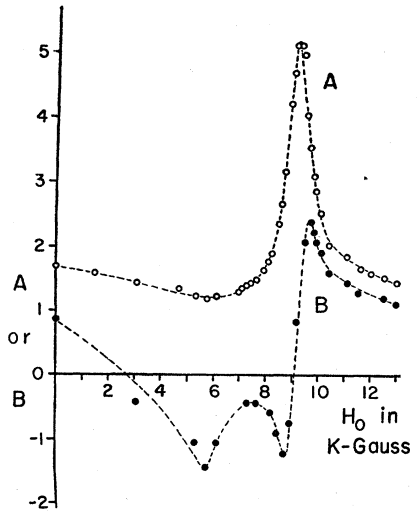

FIG. 2. Nickel perpendicular field case.

(b) Over-All Shape of Resonance Curves

Values of Q and $\Delta\omega$ are measured with respect to the appropriately chosen reference point as discussed in Sec. III. Since Q_0 enters here only as a normalization constant we will plot values of A and B as a function of the applied constant field H_0. $A=(\mu_R)^{\frac{1}{2}}$ and $B=(\pm)(\mu_L)^{\frac{1}{2}}$ for parallel magnetization, and $A=\frac{1}{2}[(\mu_R{}^+)^{\frac{1}{2}}+(\mu_R{}^-)^{\frac{1}{2}}]$ and $B=\frac{1}{2}[(\pm)(\mu_L{}^+)^{\frac{1}{2}}+(\mu_L{}^-)^{\frac{1}{2}}]$ for perpendicular magnetization. All measurements are at an rf frequency of approximately 9200 Mc/sec, the exact frequency in each case being determined by the cavity resonance.

The experimental results for nickel and supermalloy and for the cases of parallel and perpendicular magnetization are shown in Figs. 1, 2, 3, and 4.

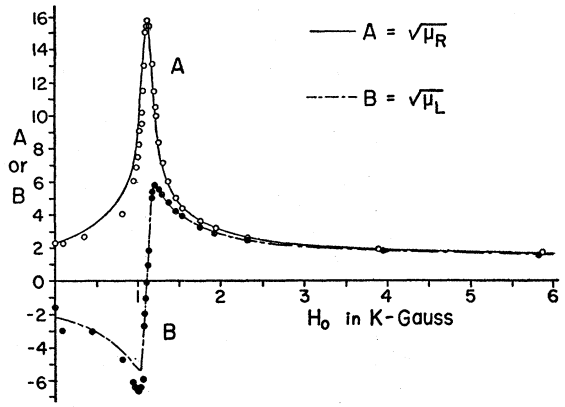

FIG. 3. Supermalloy parallel field case and comparison with theory.

We will use our measurements on supermalloy as the basis for a discussion of line shape. Exactly similar results are obtained in the case of nickel. In both cases the results depend on heat treatment and surface polishing. These effects are particularly pronounced in the case of nickel and in the measurements of frequency shift for perpendicular magnetization. They are not, however, the object of the present study and consequently we now restrict the discussion to uniformly prepared specimens of the metal supermalloy.

We consider first the case of parallel magnetization. The usual theory does not differ from the present analysis in this case, both leading to Eqs. (26a) and (26b). These equations with $\theta=0$ are plotted as continuous solid and dotted line curves in Fig. 3 for comparison with the experimental data. Bloch damping has been assumed and $1/T_2$ has been set equal to 1.7×10^9 sec^{-1}. The agreement between theory and experiment is almost as good as could be desired.

We consider next the case of perpendicular magnetization. The experimental values of A and B given in

Fig. 4 are now transferred to Figs. 5 and 6, respectively, where they are plotted against $H_0-4\pi M_0$. The dotted and solid line curves given for comparison are the theoretical curves as obtained from the usual theory in terms of demagnetization factors and the present theory leading to Eqs. (33a) and (33b). We note the following:

(1) Insofar as absorption is concerned the present theory gives results in almost perfect agreement with the experimental data. On the other hand the usual theory leads to a curve which differs from the experimental curve in two important respects. It possesses a minimum which is not observed in these X-band measurements and the curve is too wide in the neighborhood of the resonance point.

(2) Insofar as frequency shift is concerned the present theory predicts correctly the rate of frequency change near resonance together with the correct peak-

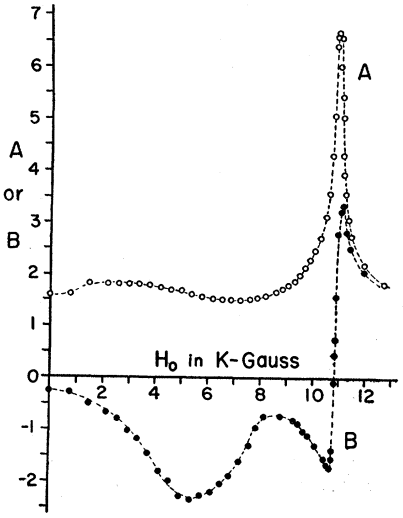

FIG. 4. Supermalloy perpendicular field case.

to-peak values. However, there are discrepancies in details of the B curve which remain to be discussed.

The minimum in the absorption which is predicted by the usual theory is a consequence of the fact that μ_1 goes through zero and remains negative over a certain portion of the range of H_0 below resonance. In the case of perpendicular magnetization it predicts that this minimum should occur at

$$(H_0-4\pi M_0)=2\pi M_0[(1+\eta^{-2})^{\frac{1}{2}}-1]\cong 1100 \text{ gauss},$$

for supermalloy at X-band frequencies. The prediction with respect to a minimum in the absorption which is made by the present theory differs in two respects. In the first place only μ_1^+ can become negative and consequently the minimum, if present, is less marked than in the usual theory. In the second place it occurs for a different value of H_0 than that given by the usual theory. According to Eq. (28) the minimum should

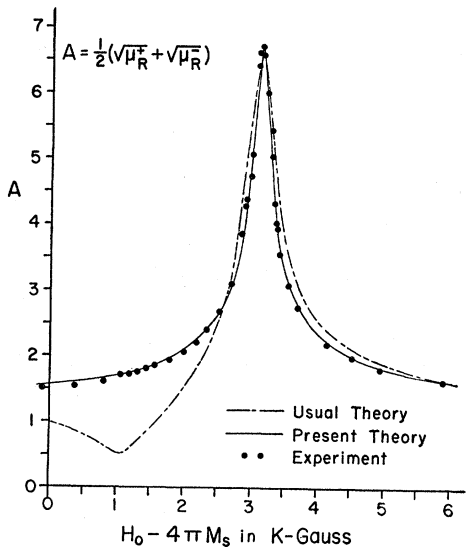

FIG. 5. Experimental and theoretical values of A in the supermalloy perpendicular field case.

occur at a value of H_0 which is approximately given by

$$(H_0-4\pi M_0)=(\omega/\gamma)-4\pi M_0.$$

Thus it will not be observed at X-band frequencies for which $\omega/\gamma\sim 4000$ gauss and $4\pi M_0\sim 7700$ gauss, but a small minimum might be detectable at K-band frequencies. This has not been observed.[12] The failure to detect a minimum in the absorption at perpendicular magnetization in our measurements at X-band frequencies as well as in previous measurements was one of the indications that the usual theory was inadequate.

(c) Details in Shape of the Resonance Curves

The data are actually of sufficient accuracy to permit a closer examination of the agreement between experimental and predicted curve shapes. We can, for example, attempt to make independent determinations

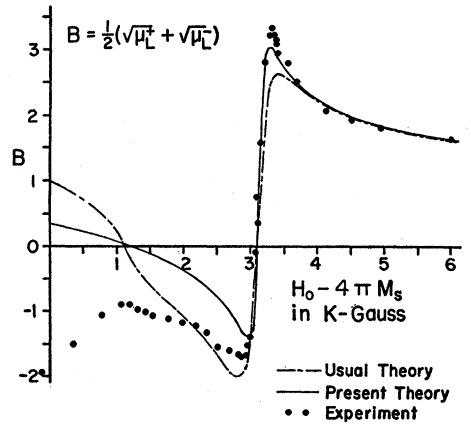

FIG. 6. Experimental and theoretical values of B in the supermalloy perpendicular field case.

of the value of the time constant T_2 by relating it to critical parameters of the resonance curves. Four such parameters are: (a) the absorption at resonance, (b) the width of the absorption curve at half-maximum, (c) the peak-to-peak value of the frequency shift, (d) the separations in the peak-to-peak values. When this is done an over-all spread of about a factor 2 is obtained in the various determinations of T_2. Some of this spread is probably due to errors in the determination of some of the critical points, e.g., the positions of maximum positive and negative frequency shift. The spread may possibly be reduced by a better choice of Q_0. However, much of it appears to be inherent and to be related more sensitively to the frequency shift curve than to the absorption curve. At the present time we are able to conclude only that the experimental methods used provide a rather stringent test of the phenomenological theory which may not be completely adequate for a precise quantitative description.

Other features of the resonance curves which remain unexplained are in the low field region. For example, in Figs. 2 and 4 we observe a second minimum in the frequency shift curve occurring at about 5700 gauss for nickel and 5500 gauss for supermalloy. Since these are perpendicular field cases, we are here in the region of unsaturated magnetization. The theory is consequently unable to explain the phenomena in question and it is for this reason that the data of Fig. 4 were replotted in Figs. 5 and 6 only for values of H_0 greater than $4\pi M_0$.

PHYSICAL REVIEW VOLUME 94, NUMBER 3 MAY 1, 1954

Theory of Boundary Effects of Superconductors*

J. BARDEEN
University of Illinois, Urbana, Illinois
(Received January 27, 1954)

An extension of the phenomenological London equations to take into account a space variation of the concentration of superconducting electrons is presented. The theory differs from that of Ginsburg and Landau in that it makes use of the Gorter-Casimir two-fluid model rather than an order parameter to derive an expression for the free energy. An effective wave function is used for the superconducting electrons. The theory is applied to calculate the boundary energy between normal and superconducting phases and the relative change $\Delta\lambda/\lambda$ of penetration depth with magnetic field. Calculated values of boundary energies are somewhat larger, and of $\Delta\lambda/\lambda$ somewhat smaller, than observed. It is suggested that additional nonlinear terms are required to account for the observed $\Delta\lambda/\lambda$ at low temperatures. The connection of the theory with Pippard's ideas on range of order is discussed briefly.

I. INTRODUCTION

TO estimate the energy of the boundary between normal and superconducting phases and for related problems, it is necessary to have a theory which takes into account a space variation in the effective concentration of superconducting electrons n_s. Across such a boundary, n_s changes from an equilibrium value on the superconducting side to zero on the normal side. We present here a theory based on the Gorter-Casimir[1] two-fluid model. It is an extension of the Ginsburg-Landau theory[2] so as to apply over the entire temperature range.

The theory of Ginsburg and Landau (denoted here by G-L) applies for temperatures close to the critical temperature T_c. These authors identify n_s with an order parameter η which is small near T_c. The free energy is expanded in a power series in η. It is assumed that n_s (and thus η) is given by the square of an effective wave function $\Psi(x)$, and that there is an energy term proportional to $|\text{grad}\Psi|^2$. The coefficient of $|\text{grad}\Psi|^2$ is evaluated in terms of the critical field H_c and the penetration depth, λ, so that there are no undetermined parameters. In addition to the calculation of the boundary energy, the theory was applied to the magnetic and thermal properties of thin films and to estimate the change in λ with magnetic field.

Using a microwave method, Pippard[3] has shown that for tin the change in λ with field is no more than 3 percent for fields up to $H=H_c$. From these results he estimated that the ordered regions must extend over distances of the order of 10^{-4} cm. Presumably the width of the normal-superconducting boundary is at least of this order.

The author[4] has pointed out that Pippard's result is

* Most of the results reported here were obtained in 1951 and 1952. The work was started while the author was employed at the Bell Telephone Laboratories and continued at the University of Illinois. At the latter institution, the work was supported in part by the Office of Ordnance Research of the U. S. Army Ordnance Corps.

[1] C. J. Gorter and H. B. G. Casimir, Physik Z. **35**, 963 (1934); Z. tech. Phys. **15**, 539 (1934). See D. Shoenberg, *Superconductivity* (Cambridge University Press, Cambridge, 1952), second edition, Chap. VI.

[2] V. L. Ginsburg and L. D. Landau, J. Exptl. Theoret. Phys. (U.S.S.R.) **20**, 1064 (1950).

[3] A. B. Pippard, Proc. Roy. Soc. (London) **A203**, 210 (1950).

[4] J. Bardeen, Phys. Rev. **81**, 1070 (1951).